*Journal of the Korean Nuclear Society*
*Volume 28, Number 3, pp. 320~330, June 1996*

# Extensions of Streaming Rays Method for Streaming Dominant Neutron Transport Problems

**Ser Gi Hong and Nam Zin Cho**
Korea Advanced Institute of Science and Technology
Department of Nuclear Engineering
373-1 Kusong-dong, Yusong-gu, Taejon 305-701, Korea

(Received February 2, 1996)

## Abstract

The streaming rays(SR) method is improved and extended to multigroup, anisotropic scattering, and three-dimensional angular space(x-y-z(infinite))problems. This method is applied to the shielding problems in which the ray effect occurs seriously. For verification, the results of MORSE-CG code are used as reference solution and the results of TWODANT code are compared. The results show that solutions of the SR method are much better than those of the TWODANT code and are in good agreement with those of the MORSE-CG code. Also, to reduce computing time, two acceleration algorithms are implemented in the SR method : the standard coarse-mesh rebalance and a new angular two-grid acceleration.

## 1. Introduction

Although the discrete ordinates method ($S_N$ method) has been effectively used in various neutron transport calculation, the method is difficult to apply to complex geometries and can be subject to the ray effect [1]. The term ray effect refers to the anomalous scalar flux distortion that appears when the conventional discrete ordinates method is applied to certain problems having strong absorbers and localized sources. The problems with isolated sources in absorbing media are encounted in shielding calculations where streaming from isolated sources is dominant. The ray effect is due to the discretization of angular variable of the transport equation in the discrete ordinates approximation, that is to say, destruction of rotational invariance of the transport equation. In the problem that has a localized source in a streaming dominant medium, the edge flux is mainly ascribed to the uncollided neutrons from the source and the flux distribution is highly peaked.

In the $S_N$ method, the ray effect occurs because of two reasons ; the one is inability of estimating the flux contributing to streaming, and the other is inability of quadrature formula in approximating reasonably the scalar flux from the discrete angular fluxes by using proper angular weights. Consequently, many efforts to mitigate this defect have been made and applied to the previous codes. Monte Carlo method [2] is very accurate for most problems and applicable to geometrically complicated problems but is subject to large variance for deep penetration problems and to long computing time. With a view of preserving the rotational invariance, many discrete ordinate transport equations in two dimensions equivalent to the $P_L$ approximation [1] have been developed successfully in reducing the ray effect. However, these methods have common defect that the convergence of iteration is very slow and that the computational scheme is much more difficult than that of $S_N$ method. The finite element method(FEM) approach [3] to the transport problem, where angular and spatial

variables are expanded by using piecewise linear or bilinear basis functions, have also been developed. The results of these methods show that scalar flux distribution on the edge is very smooth and undistorted, but the accuracy is very poor when low order functions of angular variables are used.

The SR method [4, 5, 6] combines the characteristic method[6] where the outgoing flux is calculated by integrating the transport equation along the characteristic line, with the conventional local mesh methods where discrete ordinate angular quadrature sets are used as in the $S_N$ method. Therefore, computational simplicity of the $S_N$ method is preserved, but the entire medium is overlaid with streaming rays for each direction. In the SR method, to improve accuracy of the streaming portion, the uncollided flux is calculated analytically by integrating transport equation along the streaming rays and the collided flux is calculated as in the $S_N$ method. Another feature of the SR method is that a finer angular quadrature set is used for the streaming portion of transport calculation than in the determination of scattering source, which provides efficient means for the ray effect for anisotropic problems.

In this paper, the SR method developed by Filippone on the basis of the characteristic methods is applied to the problems where the ray effect is serious, with extensions to multigroup, anisotropic scattering problems and to three-dimensional angular space (x-y-z(infinite)) [7]. The extension to three-dimensional angular space (x-y-z(infinite)) has significant importance for improving accuracy of the SR method. In addition, as acceleration schemes, the standard coarse-mesh rebalance is implemented and a new angular two-grid acceleration scheme is developed.

## 2. Theory and Methodology of SR Method

### 2.1. Decomposition into Uncollided and Collided Angular Fluxes

The starting equation of the SR method is the well known neutron balance equation that is used in $S_N$ method :

$$\mu_n A(\Psi_{n,i-1/2,j}-\Psi_{n,i+1/2,j}) + \eta_n B(\Psi_{n,i,j-1/2}-\Psi_{n,i,j+1/2}) + q_{n,i,j}V=\sigma_t\Psi_{n,i,j}V, \quad (1)$$

where $A$ and $B$ are surface areas of the vertical and horizontal faces of the ij'th cell, respectively. $V$ is the volume of the ij'th cell and $q_{n,i,j}$ is the total source. Subscript n denotes the direction for each streaming ray. Unlike the $S_N$ method, the interior and edge fluxes of each cell are decomposed into the uncollided and collided parts :

$$\Psi_n=\Psi_n^o+\Psi_n^c, \quad (2)$$

where the superscripts "o" and "c" indicate the cell uncollided and collided parts, respectively, and the indices i and j are suppressed. The terms "cell collided" and "cell uncollided" have meaning only in the cell. Therefore, the incoming cell collided flux is set to zero, since neutrons comprising this flux did not make collisions yet in the cell. The balance equation for the cell uncollided part becomes :

$$\mu_n A(\Psi^o_{n,i-1/2,j}-\Psi^o_{n,i+1/2,j}) + \eta_n B(\Psi^o_{n,i,j-1/2}-\Psi^o_{n,i,j+1/2})=\sigma_t V\Psi^o_{n,i,j}. \quad (3)$$

In the above equation, the source is zero, since uncollided neutrons in the cell are totally ascribed to incoming neutrons. The balance equation for the cell collided flux is obtained by subtracting Eq.(3) from Eq.(1) :

$$q_{n,i,j}V-(\mu_n A\Psi^c_{n,i+1/2,j}+\eta_n B\Psi^c_{n,i,j+1/2}) = \sigma_t\Psi^c_{n,i,j}V, \quad (4)$$

If the diamond difference approximation in the SR method :

$$\Psi^c_{n,i+1/2,j}\cong 2\Psi^c_{n,i,j}\cong\Psi^c_{n,i,j+1/2}$$

is used, the following equation is obtained :

$$\Psi^c_{n,i,j}=\frac{q_{n,i,j}V}{2\mu_n A+2\eta_n B+\sigma_t V}. \quad (5)$$

This equation always gives positive cell average flux even though diamond approximation is used. This is an important advantage of SR method since standard $S_N$ method may give negative flux under certain situations when diamond approximation is used.

To obtain uncollided flux, the characteristic form of the Eq.(3) is used :

$$\sin\theta_n \frac{d\Psi^o(p,k)}{dp} + \sigma_t \Psi^o(p,k) = 0. \quad (6)$$

where p represents coordinate of projected direction of neutron moving direction onto x-y plane, k coordinate perpendicular to $p$ and $\theta_n$ polar angle of neutron moving direction. In deriving Eq.(6), the following geometric relation is used :

$$p = s\sin\theta$$

where $s$ represents coordinate of neutron moving direction (see Fig. 1).

Integrating Eq.(6) over the mesh cell, the following equation is obtained :

$$\Psi^o_{n,i,j} = \frac{\sin\theta_n}{\sigma_t V}\int_0^{k_{max}} dk\{\Psi^o(p_{in},k) - \Psi^o(p_{out},k)\}, \quad (7)$$

where $p_{in}$ and $p_{out}$ mean incoming and outgoing p-coordinates, respectively, and $k_{max}$ is projected area of the medium on a plane perpendicular to neutron moving direction. Since the above integration cannot be performed analytically, it is approximated by using values of streaming rays as :

$$\Psi^o_{n,i,j} \cong \frac{\sin\theta_n}{\sigma_t V}\sum_{l\in ijcell} W^l(\Psi^{in}_{nl} - \Psi^{o,out}_{nl}), \quad (8)$$

where $W^l$ is spatial weight of $l'$ th streaming ray. The spatial weights are chosen so that summation of the weights is equal to $k_{max}$. The outgoing uncollided flux along the $l'$ th streaming ray is obtained by analytically integrating Eq.(6). The result is as follows :

$$\Psi^{o,out}_{nl} = \Psi^{in}_{nl} e^{-\sigma_t L^l}, \quad (9)$$

Inserting this result into Eq.(8), the equation for the cell uncollided flux becomes

$$\Psi^o_{n,i,j} \cong \frac{\sin\theta_n}{\sigma_t V}\sum_{l\in ijcell}(R^l_{n,i,j} - R^{ol}_{n,i,j}), \quad (10)$$

where

$$R^l_{n,i,j} = W^l \Psi^{in}_{n,l},\ R^{ol}_{n,i,j} = R^l_{n,i,j} e^{-\sigma_t L^l},\ W^l$$

is the spatial weight for the $l'$ th ray.

For the next cell calculation, total outgoing surface flux (collided and uncollided flux) is set to incoming surface flux for the next cell :

$$R^l_{i,j+1} = R^{ol}_{i,j} + W^l \Psi^c_{n,l}(x_i, y_{j+1/2})$$

if next cell is (i, j+1) (11)

and

$$R^l_{i+1,j} = R^{ol}_{i,j} + W^l \Psi^c_{n,l}(x_{i+1/2}, y_j)$$

if next cell is (i+1, j). (12)

Now that all the required equations are obtained, the solution of SR method can be found via the conventional scattering source iteration algorithm.

### 2.2. Angular Quadrature Set

The SR method requires a special azimuthal angles for computational simplicity but polar angles are arbitrary. The angular weights corresponding to each direction are chosen carefully since an inappropriate choice leads to inaccuracy of the solution. The

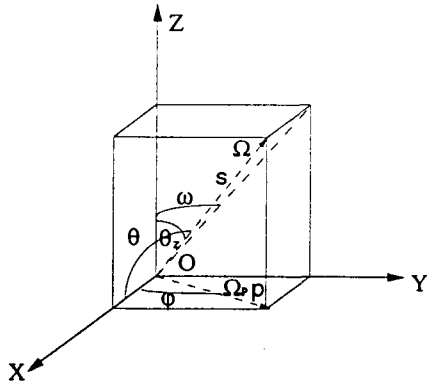


**Fig. 1. Coordinates System**

following conditions for azimuthal angles must be satisfied [4] :

$$\tan\varphi_r = (A/B)\times r/(N_\varphi+1-r), \quad r=1,2,3,\cdots,N_\varphi,$$
$$\varphi_{2N_\varphi+1-r} = \pi-\varphi_r,\ r=1,2,3,\cdots,N_\varphi,$$
$$\varphi_{2N_\varphi+r} = \pi+\varphi_r,\ r=1,2,3,\cdots 2N_\varphi, \quad (13)$$

where $N_\varphi$ is the number of azimuthal angles for an octant, with weights determined by

$$w_\varphi^1 = (\varphi_1+\varphi_2)/2,$$
$$w_\varphi^r = (\varphi_{r+1}-\varphi_{r-1})/2,\ r=2,3,4,\cdots,4N_\varphi-1,$$
$$w_\varphi^{4N_\varphi} = 2\pi-(\varphi_{4N_\varphi-1}+\varphi_{4N_\varphi})/2. \quad (14)$$

Here, the polar angles are simply determined by the following equation :

$$\xi_p = \cos\theta_p = (p-1/2)(1/N_\xi), \quad p=1,2,3,\cdots,N_\xi, \quad (15)$$

where $N_\xi$ is the number of polar angles for upper hemisphere, with uniform weights :

$$w_\theta^p = \frac{1}{N_\xi}, \quad p=1,2,3,\cdots,N_\xi. \quad (16)$$

The total weights are products of the azimuthal and polar weights. These total weights are normalized so that the summation is unity.

The numerical results we obtained show that the shape of the edge flux distribution depends mainly on the number of azimuthal angles and associated weights, while amplitude of the distribution depends on the number of polar angles and polar weights. For most problems, only two polar angles in half hemisphere are sufficient.

### 2.3. Scattering Source

The directions of the streaming rays need not to correspond to directions used to describe the angular fluxes and sources. In SR method, a finer angular quadrature set is used to calculate the streaming component than that used in determination of the source. In this treatment, the fine angular fluxes are not saved, but used only in forming the coarse angular fluxes. Therefore, this leads to large savings in computer storage requirement without significantly affecting accuracy of the calculation. The scattering source for m'th angular group is given by

$$S_{mg} = \sum_{n\in m}\omega^n S_g^n \quad (17)$$

where

$$S_g^n = \sum_{g'=1}^{G}\sum_{n'=1}^{N}\omega^{n'}\sigma_{sgg'}(n'\to n)\Psi_{g'}^{n'} \quad (18)$$

Defining

$$\sigma_{mm'gg'} = \frac{\sum_{n'\in m'}\omega^{n'}\sum_{n\in m}\omega^n\sigma_{sgg'}(n'\to n)\Psi_{g'}^{n'}}{\sum_{n'\in m'}\Psi_{g'}^{n'}} \quad (19)$$

and approximating this equation under the assumption that the number of angular groups($M$) is chosen large enough to adequately represent the anisotropy of the scattering kernel, the following equation is obtained :

$$\sigma_{mm'gg'} = \sum_{n'\in m'}\sum_{n\in m}\omega^{n'}\omega^n\sigma_{sgg'}(n'\to n).$$

Then, Eq.(18) becomes

$$S_{mg} \cong \sum_{g'=1}^{G}\sum_{m'=1}^{M}\sigma_{mm'gg'}\Psi_{m'g'}, \quad (20)$$

where

$$\Psi_{mg} = 1/\omega_m\sum_{n\in m}\omega^n\Psi_g^n \quad \text{and} \quad \omega_m = \sum_{n\in m}\omega^n.$$

Finally, the scattering source for the streaming ray is given by

$$S_g^n \cong \frac{S_{mg}}{\omega_m}, \quad n\in m.$$

For isotropic scattering problems, this treatment is exact. However, for anisotropic scattering problems, the scattering cross section can be expanded by using Legendre polynomials. For example, in case of linearly anisotropic scattering, the scattering cross section is given by the following equation :

$$\sigma_{mm'gg'} = \sum_{n'\in m'}\sum_{n\in m}\omega^{n'}\omega^n(\sigma_{sgg'0}+3\sigma_{sgg'1}\mu_0(n,n'))$$

$$= \sigma_{sgg'0}\,\omega_{m'}\omega_m + 3\sigma_{sgg'1}\sum_{n'\in m'}\sum_{n\in m}\mu_0(n,n')\,\omega^{n'}\omega^n, \quad (21)$$

where $\mu_0(n, n')$ is cosine of the angle between direction $\hat{\Omega}_{n'}$ and $\hat{\Omega}_n$

### 3. Acceleration of SR Method

Since the SR method requires more arithmetic operations than $S_N$ method for each iteration, the corresponding computing time is longer. Therefore, implementation of acceleration scheme in the SR method is needed. The potentially most effective acceleration methods used to date are coarse-mesh rebalance methods and diffusion synthetic methods. In particular, the diffusion synthetic acceleration (DSA) [8, 9, 10] is a powerful scheme for the $S_N$ method, but it is not considered in this study since the stable difference scheme of the diffusion equation is difficult to find. In this study, a simple angular two-grid acceleration method is developed as an alternative to the DSA scheme, to avoid the algebraic complexities related with the derivation of the DSA equation and the standard coarse-mesh rebalance method is implemented. It is well known that, to have a stable DSA scheme, the DSA equation must be derived from the discretized transport equation [8, 9], but this derivation is extremely difficult to perform in higher-order differencing schemes and in multidimensional problems. On the other hand, the coarse-mesh acceleration method is applicable to any transport problems with balance equation. But it requires more iterations than the DSA scheme and has instabilities in optically thick problems. The angular two-grid acceleration method uses a transport equation of lower order as the lower operator to reduce the error. Since our angular two-grid acceleration method uses simply less number of discrete angles, the implementation is very simple and the instability does not occur. But a longer time is required to solve the diffusion equation in DSA. This method is described only in one-dimensional geometry with isotropic scattering but various numerical tests are performed in x-y geometry. The one-dimensional transport equation for isotropic scattering medium is as follows :

$$\mu_n\frac{\partial\,\tilde{\Psi}^{n,\,l+1/2}}{\partial x} + \tilde{\Psi}^{n,\,l+1/2} = c\,\phi_0^l + S^n \quad (22)$$

and

$$\phi_0^l = \sum_m \omega_m \Psi_m^l, \quad m = 1, 2, 3, \cdots, M, \quad (23)$$

where $c$ is the ratio of scattering to total cross section and, for convenience, $\sigma_t$ is set to unity. If we consider Eq.(22) only for the coarse angular set($C_o$), where its element is denoted by subscript $a$, we obtain

$$\mu_a\frac{\partial\,\tilde{\Psi}^{a,\,l+1/2}}{\partial x} + \tilde{\Psi}^{a,\,l+1/2} = c\,\phi_o^l + S^a, \quad a\in Co. \quad (24)$$

Also, the equation with source $c\tilde{\phi}_0^{l-1/2}$ can be written as follows :

$$\mu_a\frac{\partial u^{a,\,l+1/2}}{\partial x} + u^{a,\,l+1/2} = c\,\tilde{\phi}_0^{\,l+1/2} + S^a, \; a\in Co \quad (25)$$

Subtracting Eq.(25) from Eq.(24), we obtain

$$\mu_a\frac{\partial C^{a,\,l+1/2}}{\partial x} + C^{a,\,l+1/2} = c(\,\tilde{\phi}_0^{\,l+1/2} - \phi_0^l), \quad (26)$$

where

$$C^{a,\,l+1/2} = u^{a,\,l+1/2} - \tilde{\Psi}^{a,\,l+1/2}. \quad (27)$$

We define the angular group correction as follows :

$$C_m^{l+1/2} \equiv \frac{1}{\omega'_m}\sum_{a\in m}\omega^a C^{a,\,l+1/2}, \quad (28)$$

where

$$\omega'_m = \sum_{a\in m}\omega^a. \quad (29)$$

The angular group flux is updated as follows :

$$\Psi_m^{l+1} = \tilde{\Psi}_m^{\,l+1/2} + \vartheta C_m^{l+1/2}, \quad (30)$$

where the relaxation factor $\theta$ is chosen so that the number of iterations is minimized. Finally, the scalar flux is updated as follow :

$$\phi_0^{l+1} = \tilde{\phi}_0^{\,l+1/2} + \vartheta C^{l+1/2}, \quad (31)$$

where

$$\tilde{\phi}_0^{l+1/2} = \sum_n \omega^n \tilde{\Psi}^{n,\,l+1/2}, \tag{32}$$

and

$$C^{l+1/2} = \frac{\omega_1}{\omega'_1} \sum_{a \in Co} \omega^a C^{a,\,l+1/2}. \tag{33}$$

In Eqs.(32) and (33), we assumed that there is only one angular group per octant.

We analyze eigenvalues of this acceleration method for infinite system by using the following Fourier Ansatz [10] :

$$\begin{aligned} \phi_0^l &= e^{j\lambda x}, \\ \tilde{\Psi}^{n,\,l+1/2} &= t^n e^{j\lambda x}, \\ C^{a,\,l+1/2} &= C^a e^{j\lambda x}, \\ \tilde{\phi}_0^{l+1/2} &= \sum_n \omega^n t^n e^{j\lambda x}, \\ C^{l+1/2} &= \frac{\omega_1}{\omega'_1} \sum_{a \in Co} C^a \omega^a e^{j\lambda x}, \\ \phi_0^{l+1} &= \omega e^{j\lambda x}, \\ S^a &= S^n = 0. \end{aligned} \tag{34}$$

Substituting Eq.(34) into Eq.(22), we obtain

$$t^n = \frac{c}{1 + j\lambda\mu_n} \tag{35}$$

and substituting Eq.(34) into Eq.(26), we obtain

$$C^a = \frac{c}{1 + j\lambda\mu_a} \left( \sum_n \omega^n t^n - 1 \right). \tag{36}$$

Finally, substituting Eqs.(34), (35), and (36) into Eq. (31),

we obtain

$$\omega = c \left\{ \sum_{n=1}^{M} \frac{\omega^n}{1 + \lambda^2 \mu_n^2} \left[ 1 + \frac{\omega_1}{\omega'_1} \vartheta \sum_{a \in Co} \frac{\omega^a C^a}{1 + \lambda^2 \mu_a^2} \right] - \frac{\omega_1}{\omega'_1} \vartheta \sum_{a \in Co} \frac{\omega^a}{1 + \lambda^2 \mu_a^2} \right\}. \tag{37}$$

## 4. Application and Numerical Results

Three benchmark problems, which are well known to be difficult in shielding problems, are chosen to compare results of SR method with those of other methods. The numerical results are compared with those of the well known two codes : MORSE-CG [2] and TWODANT [11]. The MORSE-CG code is the most typical Monte Carlo code. In running the MORSE-CG code for all problems in this study, to represent the infiniteness of z-direction, the length of z-direction is taken large, e.g., 200 m.f.p. This results are used as reference solutions. And the TWODANT code is used to obtain results of $S_N$ method. In this study, scalar flux (neutrons/$cm^2$ sec) distribution on the edge is the quantity of interest to show reduction of the ray effect. In all results, the order of SR method is denoted by $SR_{N_\phi,\,N_\xi,\,M_\phi,\,M_\xi}$ where $M_\phi$ is the number of coarse azimuthal angular groups and $M$ the number of coarse polar angular groups for an octant.

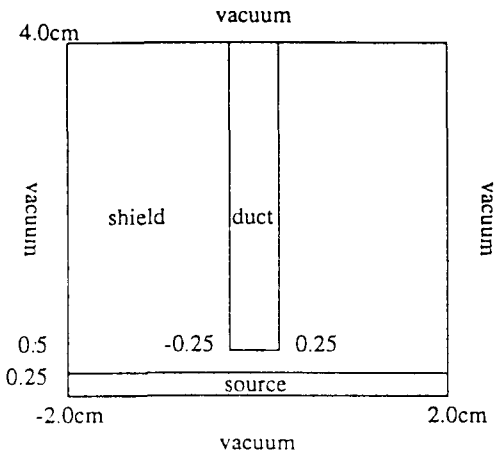


**Fig. 2. Configuration of the Benchmark Problem I**

**Table 1. Cross Sections($cm^{-1}$) and Sources of the Benchmark Problem I**

| cross section | group 1 | group 2 |
|---|---|---|
| $\sigma_a$ | 0.0600 | 0.0960 |
| $\sigma_f$ | 0.0000 | 0.0000 |
| $\sigma_t$ | 0.0930 | 0.1080 |
| $\sigma_{s0g\cdot g}$ | 0.0100 | 0.0120 |
| $\sigma_{s0g\cdot 1-g}$ | | 0.0230 |
| $\sigma_{s1g\cdot g}$ | 0.0089 | 0.0039 |
| $\sigma_{s1g\cdot 1-g}$ | | 0.0090 |
| source($n/cm^3$sec) | 0.2000 | 2.0000 |

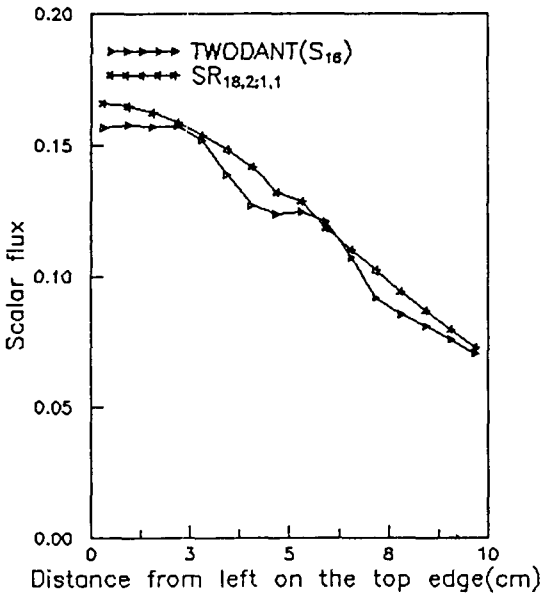


**Fig. 3. Configuration of the Benchmark Problem I (group 1 flux)**

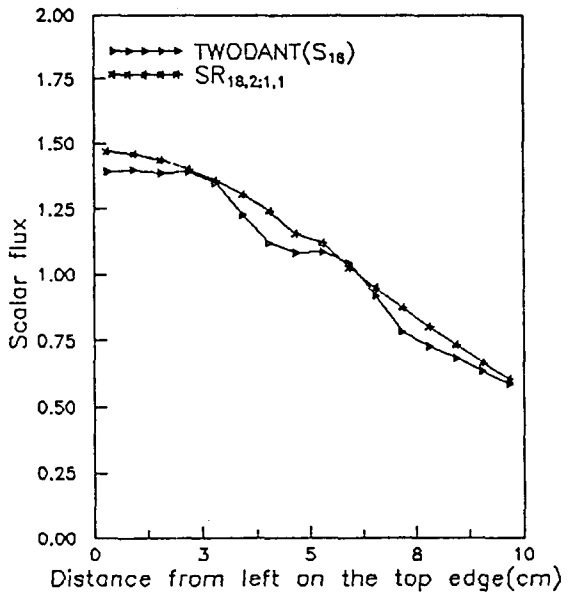


**Fig. 4. Result of the Benchmark Problem I(group 2 flux)**

### 4.1. Benchmark Problem I

This benchmark problem was chosen for the purpose of testing the capability of SR method that estimates the flux in two group, linearly anisotropic scattering problem. The configuration of this benchmark problem (see Fig. 2) is well known and this problem has been dealt in many studies to analyze the ray effect of discrete ordinate transport calculation. Informations for the cross sections are given in Table 1. The problem domain is divided into $16\times16$ meshes. The results of this benchmark problem are shown in Fig. 3 (for the fast flux) and 4 (for the thermal flux). The results show that the ray effect is significantly reduced in comparison with the TWODANT code.

### 4.2. Benchmark Problem II

This benchmark problem models a duct (0.5cm width) in a shield to estimate the leakage of the neutrons through the duct, since streaming ducts in shields are a common design problem for which empirical rules of thumb are often used. The configuration of this benchmark problem is given in Fig. 5 and the cross sections are given in Table 2. The domain of the problem is divided into $16\times16$ meshes (by symmetry about $x=0$, only the left half of the problem is actually solved) and the cell average fluxes along the uppermost row of mesh cells are estimated. Since a vacuum duct is nearly penetrated into the shield region, it is expected that the main leakage through the top surface is ascribed to streaming of neutrons through the duct. Therefore, the capability that estimates the streaming component is very important in obtaining the accurate solution. Since the SR method calculates the uncollided flux by analytically integrating the transport equation, the estimation of the streaming component is very accurate and thus the ray effect is strongly ameliorated in the overall region, as shown in Fig. 6. In particular, the solution in the vacuum region shows good agreement with that of the MORSE-CG code while the TWODANT code does not only give seriously distorted solution

but also significantly underestimated solution.

To show the improvement of accuracy with extension to the three-dimensional angular quadrature set, the above result is compared with that obtained on the assumption that neutrons move only on the plane. As shown in Fig. 6, although the SR method with two-dimensional angular quadrature set provides quite good flux distribution in the vacuum region, the accuracy in the shield region is highly degraded in comparison with that of SR method with three-dimensional angular quadrature set. It is thus indispensable that the three-dimensional angular quadrature set is needed.

### 4.3. Benchmark Problem Ⅲ

This benchmark problem is the most difficult one among the problems chosen in this study. Fig. 7 shows the configuration of this problem, where a square source is surrounded by a void, which is in turn surrounded by a purely absorbing medium and then free space (i.e., vacuum). It is expected that the ray effect occurs seriously due to the internal vacuum duct. The problem domain is divided into $16\times16$ meshes and the flux distribution along the uppermost rows is given in Fig. 8. The local ray effect is observed near the center region in SR method, while more serious fluctuation is observed in the entire region in the result of the TWODANT code. Also the rise of the flux in the vicinity of the boundary is noted in the TWODANT solution. This behavior is mainly due to the existence of the internal vacuum outside of the source. For mitigation of this local ray effect, a larger number of polar angles are required in SR method.

### 4.4. Acceleration

The two acceleration methods are applied to Benchmark Problem Ⅱ (with differing, wider duct of 1 cm) for the reduction of computing time. The optimal relaxation factor $\theta_{opt}$ in angular two-grid acceler-

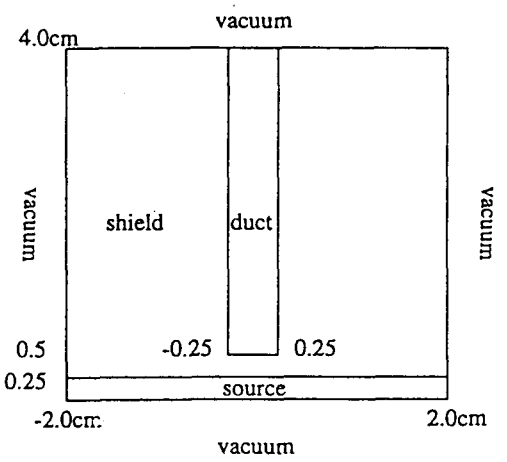


**Fig. 5. Configuration of the Benchmark Problem Ⅱ**

**Table 2. Cross Sections($cm^{-1}$) and Sources of the Benchmark Problem Ⅱ, Ⅲ**

| cross sections | benchmark problem Ⅱ | | benchmark problem Ⅲ | |
|---|---|---|---|---|
| | shield | duct | shield | duct |
| $\sigma_a$ | 0.75 | 0.00 | 0.80 | 0.00 |
| $\sigma_f$ | 0.00 | 0.00 | 0.00 | 0.00 |
| $\sigma_t$ | 1.00 | 0.00 | 0.80 | 0.00 |
| source ($n/cm^3sec$) | 2.00 | | 6.40 | |

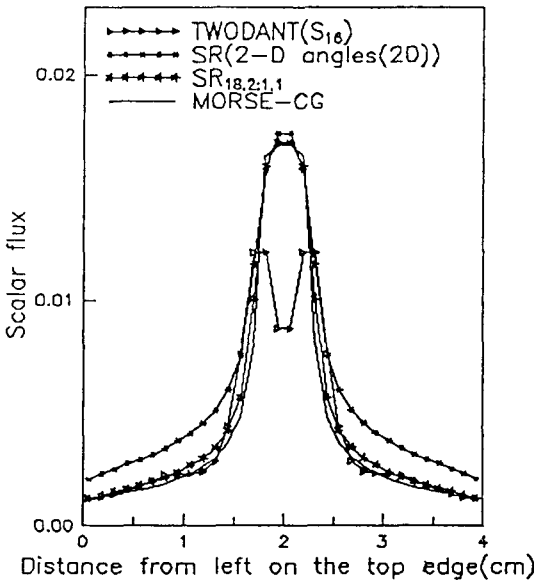


**Fig. 6. Result of the Benchmark Problem Ⅱ**

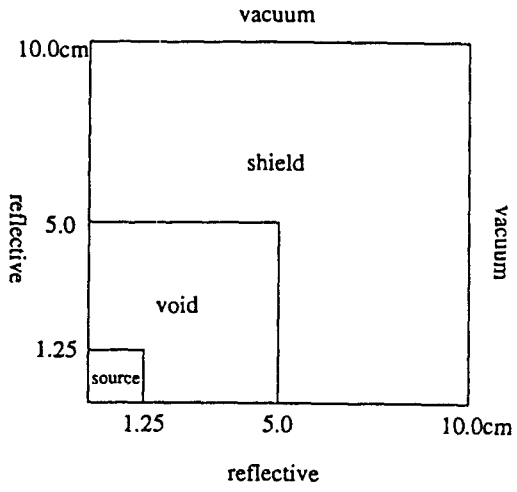


**Fig. 7. Configuration of the Benchmark Problem III**

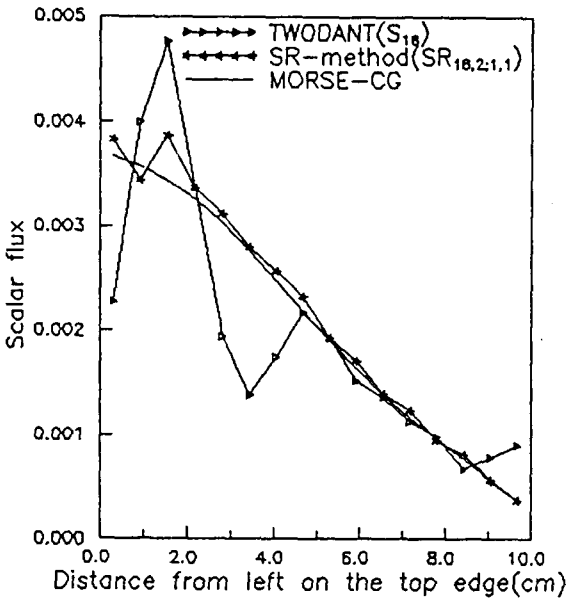


**Fig. 8. Result of the Benchmark Problem III**

ation scheme is numerically searched. To give insight into the convergency of angular two-grid acceleration scheme, the eigenvalue distributions are found by Fourier analysis. Fig. 9 shows the eigenvalue distributions obtained by Fourier analysis, where the discrete ordinates in $S_2$ is used as the coarse set and the ratio $c=0.5$. Two coarse angular set ($SR_{1,1}$, $SR_{N_p/2,N_t}$) are tested to show that a set with only one angle per octant can be effectively used as the coarse angular set. That is to say, although numbers of iterations for the two sets are nearly the same, the computing time required in the case that $SR_{1,1}$ angular set is used is much shorter than that of the other case. The computing time achieved with the two coarse angular sets is compared with that of coarse-mesh rebalance acceleration in Tables 3 and 4. Note that the computing time is comparable to that of coarse mesh rebalance acceleration. In all calculations above, the following convergence criterion for the scalar flux is used:

$$\max\left|\frac{\phi_{ij}^{l}-\phi_{ij}^{l-1}}{\phi_{ij}^{l}}\right|<10^{-4}, \quad \text{for all ij.} \tag{38}$$

We also compare the eigenvalue distributions for angular two-grid acceleration method with that for $P_1$ synthetic acceleration method. Fig. 10 shows the eigenvalue distributions for $c=0.5$. From this figure it is observed that the spectral radius of angular two-grid acceleration is comparable to that of $P_1$ synthetic acceleration for $c<0.5$.

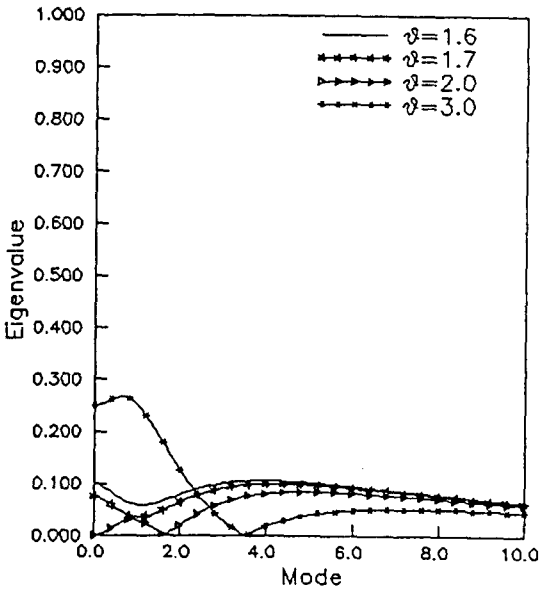


**Fig. 9. Eigenvalue Distributions for $\theta$ values (c=0.5)**

**Table 3. Comparison of Computing Times (c=0.5)**

| methods | | number of iterations | computing times[a] (sec) |
|---|---|---|---|
| no acceleration(SR[18,2,1,1]) | | 17 | 334.3 |
| AMG[b] | SR[9,2] | 7 | 197.6 |
| coarse set | SR[1,1] | 8 | 155.5 |
| CMR[c] | 8(2)×16(2)[d] | 8 | 165.5 |
| coarse mesh | 4(4)×8(4) | 8 | 156.6 |
| | (12,4)×(4,28)[e] | 11 | 209.6 |

[a]SUN SPARC2 is used
[b]angular multigrid acceleration, [c]coarse mesh rebalance method
[d]a(A)xb(B) : a-number of coarse meshes on the x-axis
A-number of fine meshes for each coarse mesh
b-number of coarse meshes on the y-axis
B-number of fine meshes for each coarse mesh
[e](a,b)x(c,d) : a-number of fine meshes in the first coarse mesh on the x-axis
b-number of fine meshes in the second coarse mesh on the x-axis
c-number of fine meshes in the first coarse mesh on the y-axis
d-number of fine meshes in the second coarse mesh on the y-axis

**Table 4. Comparison of Computing Times (c=0.9)**

| methods | | number of iterations | computing times (sec) |
|---|---|---|---|
| no acceleration(SR[18,2,1,1]) | | 35 | 699.4 |
| AMG | SR[9,2] | 12 | 338.3 |
| coarse set | SR[1,1] | 13 | 252.3 |
| CMR | 8(2)×16(2) | 10 | 206.8 |
| coarse mesh | 4(4)×8(4) | 8 | 176.0 |
| | (12,4)×(4,28) | 16 | 302.4 |

## 5. Conclusions

In this study, Filippone's SR method, a class of characteristic methods is applied to several streaming dominant problems in which the ray effect occurs seriously, with extensions to multigroup, linearly anisotropic scattering, and three-dimensional angular space(x-y-z(infinite)) treatments for the purpose of improving generality and accuracy. For verification, the results of MORSE-CG code are used as reference solution. The solution of $S_N$ method is obtained by using the TWODANT code. The results show that the solutions of SR method are in good agreement

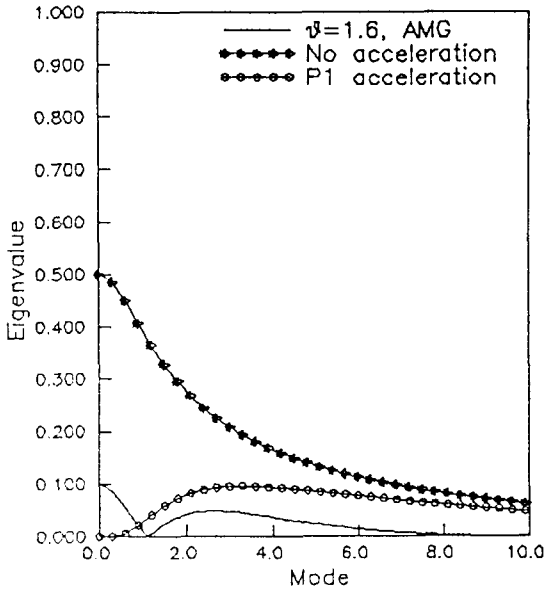


**Fig. 10. Comparison of Eigenvalue Distributions (c=0.5)**

with those of the MORSE-CG code for most benchmark problems considered, and the ray effect is significantly reduced. In particular, it is noted that the solution of SR method is very accurate in the vacuum duct region. Also, to reduce the computing time, two acceleration methods are applied to the SR method. One is the standard coarse-mesh rebalance acceleration and the other is a new angular two-grid acceleration. The implementation of the angular two-grid acceleration is very simple and the computing time is comparable to that of the coarse-mesh rebalance acceleration. In particular, it is worthwhile to note that the spectral radius of the angular two-grid acceleration is smaller than that of $P_1$ synthetic acceleration for streaming dominant problems ($c<0.5$).

## References

1. W.F. Miller, Jr., and Wm. H. Reed, "Ray Effect Mitigation Methods for Two-Dimensional Neutron Transport Theory," Nucl. Sci. Eng., **62**, 391~411 (1977)

2. M.B. Emmett, "The MORSE Monte Carlo Radiation Transport Code System," ORNL-4972, Oak Ridge National Laboratory (1975)
3. L.L. Briggs, W.F. Miller, Jr., and E.E. Lewis, "Ray-Effect Mitigation in Discrete Ordinate-Like Angular Finite Element Approximations in Neutron Transport," Nucl. Sci. Eng., **57,** 205~217 (1975)
4. W.L. Filippone, S. Woolf, and R. Lavigne, "Particle Transport Calculations with the Method of Streaming Rays," Nucl. Sci. Eng., **77,** 119~136 (1981)
5. W.L. Filippone, S. Woolf, "Application of the Method of Streaming Rays to Particle Transport in Complex Geometries," *Proc. Int. Topl. Mtg. Advances in Mathematical Methods for the solution of Nuclear Engineering Problems,* Munich, Vol. 1, p. 67 (1981)
6. R.E. Alcouffe and E.W. Larsen, "A Review of Characteristic Methods Used to Solve the Linear Transport Equation," *Proc. Int. Topl. Advances in Mathematical Methods for the Solution of Nuclear Engineering Problems,* Munich, FRG, April 27~29, 1981, American Nuclear Society (1981)
7. S.G. Hong, "An Investigation of the Method of Streaming Rays for Radiation Transport Problems," MS Thesis, Department of Nuclear Engineering, KAIST, February (1994)
8. E.W. Larsen, "Unconditionally Stable Diffusion-Synthetic Acceleration Methods for the Slab Geometry Discrete Ordinates Equations," Nucl. Sci. Eng., **82,** 47~63 (1982)
9. R.E. Alcouffe, "Diffusion Synthetic Acceleration Methods for the Diamond Differenced Discrete-Ordinates Equations," Nucl. Sci. Eng., **64,** 344~355 (1977)
10. D. Valougeorgis, M. Williams, and E.W. Larsen, "Stability Analysis of Synthetic Acceleration Methods with Anisotropic Scattering," Nucl. Sci. Eng., **99,** 91~98 (1988)
11. R.E. Alcouffe et el., "User's Guide for TWOD-ANT : A Code Package for Two-Dimensional, Diffusion-Accelerated, Neutral-Particle Transport," LA-10049-M, LANL (1990)